Evaluation of Crack-arrest Toughness Through Dynamic Fracture Analysis of Large Vessel Tests*

C. E. PUGH, B. R. BASS, R. H. BRYAN and J. KEENEY-WALKER

Oak Ridge National Laboratory (ORNL), Oak Ridge, TN 37831, USA

ABSTRACT

Elastodynamic fracture analysis results are summarized for an experiment that relates to nuclear reactor pressure vessel integrity assessments under pressurized-thermal-shock (PTS) conditions. The experiment (PTSE-2) represents the second in a series of large PTS experiments at the Oak Ridge National Laboratory and was designed to examine crack propagation and arrest in a material that exhibits low tearing resistance. Dynamic fracture analysis techniques are employed to interpret two cleavage crack run-arrest events observed in the test. Results from these analyses are compared with measured data and with results from a quasi-static analysis method.

KEYWORDS

Crack-arrest toughness; dynamic fracture; fracture mechanics; pressurized-thermal-shock

INTRODUCTION

The Heavy-Section Steel Technology (HSST) Program at the Oak Ridge National Laboratory (ORNL) addresses various aspects of light-water reactor (LWR) pressure vessel (RPV) integrity under accident scenarios, including PTS events. Central to these studies is understanding conditions that govern the initiation, rapid propagation, arrest, and ductile tearing of a crack in RPV steels. Inner-surface cracks in LWR pressure vessels may propagate during postulated PTS events. The technology must be available to determine whether a vessel can retain integrity after the arrest of a running crack in a region of lower load, higher temperature, or less irradiation damage.

*Research sponsored by the Office of Nuclear Regulatory Research, U.S. Nuclear Regulatory Commission under Interagency Agreements 0551-0551-A1 and 0552-0552-A1 with the U.S. Department of Energy under Contract DE-AC05-84OR21400 with Martin Marietta Energy Systems, Inc.

A primary objective of the HSST crack-arrest studies has been to obtain reliable toughness data and to develop procedures for predicting crack arrest at temperatures approaching the Charpy upper-shelf regime. Early laboratory studies by numerous investigators have led to the use of crack arrest specimens that reduce the dynamic effects of a running crack. However, these specimens provide limited constraint of deformation in the crack-plane region and a driving force that decreases with crack extension. These factors limit the generation of valid data from these specimens to temperatures below those where arrest is most likely to occur in a PTS scenario. The HSST Program is measuring crack-arrest data over an expanded temperature range through pressurized-thermal-shock tests (Bryan *et al.*, 1986, 1987) that provide validation data under multiaxial transient conditions. Additionally, the recent wide-plate tests (Naus, *et al.*, 1988) sponsored by the HSST program are providing the opportunity to obtain a more significant number of data points at affordable costs.

Crack propagation and arrest behavior has historically been interpreted and analyzed in terms of static fracture mechanics concepts. However, the events are inherently dynamic, so that the analysis methods should consider inertial and strain-rate effects that are known to be present. Accordingly, in concert with subcontracting groups, the HSST Program is supporting parallel research efforts to develop elastodynamic and viscoplastic-dynamic finite element analysis techniques (Bass *et al.*, 1988a,b) that can be applied to crack-arrest experiments. At ORNL, these techniques have been implemented in the ADINA/VPF (Bathe, 1984; Bass *et al.*, 1988b) dynamic crack analysis computer code. A summary of the elastodynamic analysis capabilities of ADINA/VPF is given in Sect. 2 of this paper.

The predictive capabilities of the techniques implemented in ADINA/VPF are being evaluated through applications to small- and large-scale HSST fracture tests, including the two PTS experiments (PTSE-1 and -2). The PTS experiments are the most recent of a long succession of fracture mechanics validation experiments that are on a sufficiently large scale to allow important aspects of the fracture behavior of nuclear reactor pressure vessels to be simulated. Elastodynamic finite element analyses (Bass *et al.*, 1987) were previously carried out for the two cleavage crack run-arrest events that occurred in the second and third phases of the PTSE-1 test (Bryan *et al.*, 1986). The dynamic results showed good agreement between data and predictions for the short crack runs of that experiment, and quasi-static and dynamic analyses showed little difference. These same dynamic fracture analysis techniques have been applied now to the analysis of the two crack run-arrest events of PTSE-2 (Bryan *et al.*, 1987). In Sect. 3 of this paper, the dynamic results are compared with measured data and with results from a quasi-static method. Finally, some conclusions are presented based on the outcome of the analyses.

DYNAMIC ANALYSIS TECHNIQUES

Elastodynamic analyses described in this paper were carried out using the ADINA/VPF dynamic crack analysis code. The code is capable of performing both application-mode (crack tip is propagated incrementally when K_I, the dynamically computed stress-intensity factor, equals the specified dynamic fracture toughness value, K_{ID}) and generation-mode (crack tip is propagated incrementally according to a prescribed crack position vs time relationship with the values of fracture toughness determined from the dynamically computed K_I) analyses. For both modes, the dynamic stress-intensity factor is determined in each time step from the dynamic J-integral containing the

appropriate inertial and thermal terms. In the crack-growth modeling technique of ADINA/VPF, the finite element immediately ahead of the crack tip is divided into N subelements (typically, N = 5-10). During propagation, the tip is moved through these subelements along the crack plane in discrete jumps. The position of the crack tip relative to these subelement divisions is determined from restraining forces which are placed on the crack-plane nodes of the element adjacent to the crack tip; these forces are released incrementally as the tip propagates through the element. The restraining forces are postulated to vary linearly with the crack-tip location within the element. For the analyses in the present study, the crack tip is propagated incrementally when K_I is equal to K_{ID}, the dynamic fracture-toughness relation that is taken to be a function of crack velocity $\dot{a}$ and temperature T.

For the PTSE-2 material, the dynamic toughness relation is taken to be

$$K_{ID} = K_{Ia} + A(\dot{a})^2 \text{ , where} \tag{1}$$

$$K_{Ia} = 34.0 + 8.647e^{0.02413T} \text{ , and} \tag{2}$$

$$A(T) = [329.7 + 16.25\ (T - DW_{NDT})] \times 10^{-6} \text{ , or} \tag{3}$$

$$A(T) = [121.71 + 1.2962\ (T - DW_{NDT})] \times 10^{-6} \text{ ,} \tag{4}$$

if $(T - DW_{NDT})$ is greater or less than -13.9°C, respectively; DW_{NDT} is taken to be 49°C. Units for K, A, $\dot{a}$, and T are MPa $m^{1/2}$, MPa s^2 $m^{-3/2}$, m/s and °C, respectively.

The importance of considering dynamic analysis methods to interpret large-scale tests is demonstrated by comparing the values given in Fig. 1 for the HSST wide-plate test WP-2.4 (Naus et al., 1988). Values of K_{Ia} determined using handbook equations [secant equation (Fedderson, 1967) and the Tada fixed-load condition (Tada *et al.*, 1973)] represent approximate lower and upper bounds, respectively, to the results, Fig. 1. For the long-durations of the crack run-arrest events (>20 ms) observed for the LUS WP-2 material, considerable load adjustment can take place as a result of specimen/pull-plate compliance. Therefore, the most meaningful calculations of K_{Ia} values under such conditions must take these factors into account through the use of a dynamic finite-element analysis. For example, dynamic generation-mode (fixed load and fixed displacement) analysis results for test WP-2.4 are also shown in Fig. 1. Note that the long fracture durations lead to dynamic results that approach those predicted by load-controlled static calculations. Results presented in Fig. 1 show that the wide-plate K_{Ia} test results for WP-2.4 exhibit an accelerating increase in arrest-toughness values with increasing temperature. This trend for K_{Ia} values extends consistently well above the limit of 220 MPa$\sqrt{m}$ provided in ASME Sect. XI, as described by Naus *et al.*, (1988).

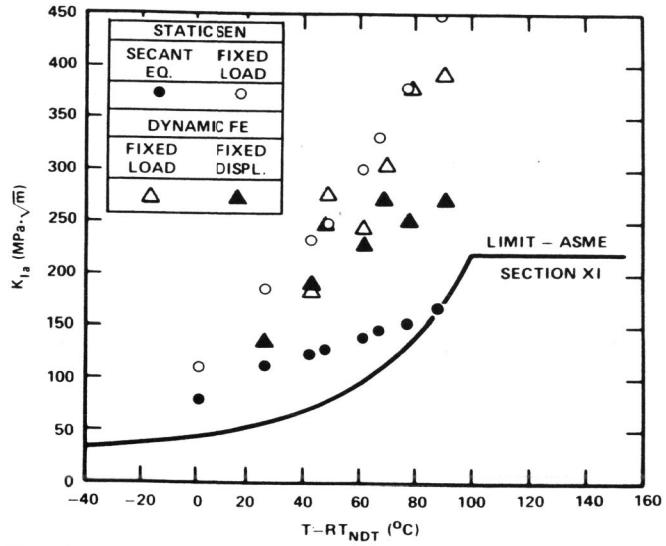

Fig. 1. Static and dynamic crack-arrest toughness determination versus temperature (T-RT$_{NDT}$) for specimen WP-2.4.

DYNAMIC FRACTURE ANALYSES OF PTSE-2

Dimensions of the test vessel and flaw geometry are given in Table 1 for the PTSE-2 test (Bryan et al., 1987). An HSST intermediate test vessel was used as a tough carrier vessel and prepared with a plug of test steel welded into the vessel. The test material was a specially heat treated 2 1/4 Cr-1 Mo plate with a low Charpy upper-shelf energy (~50 to 70 J) and low ductile-tearing resistance. The 1-m-long sharp flaw was implanted in the outside surface of the plug by cracking a shallow electron-beam weld under the influence of hydrogen charging. For each test, the vessel was extensively instrumented to give direct measurements of crack-mouth opening displacement, temperature profiles through the vessel wall, and internal pressure during the transient. In the experiment, the flawed vessel was enclosed in an outer vessel that was electrically heated to bring the test vessel to the desired uniform initial temperature of about 290°C. A thermal transient is initiated by suddenly injecting chilled water or a methanol-water mixture through an annulus between the test vessel and the

Table 1. Geometric parameters of PTSE-2 vessel

Inside radius	= 343 mm
Wall thickness (w)	= 147.6 mm
Flaw length	= 1000 mm
Flaw depth (a)	= 14.5 mm
a/w	= 0.098 mm

outer vessel. Extensive material properties tests of the vessel insert preceded the transient test of the PTSE vessel. The tensile strength was undesirably low, but other properties, although somewhat uncertain, were satisfactory. Some of the properties determined prior to the experiment are summarized in Table 2.

Table 2. Material properties of PTSE-2 vessel insert

Yield strength	= 255 MPa
Ultimate strength	= 518 MPa
NDT temperature	= 49°C
Onset of Charpy upper shelf (100% shear fracture appearance)	= 150°C
Charpy upper-shelf Energy	= 50—75J[a]

[a]Range for all depths in plate. The average at 1/4 depth is 68 J.

The experiment was planned to consist of two transients, of which the first would induce warm prestressing ($\dot{K}_I < 0$) followed by reloading ($\dot{K}_I > 0$) until the crack propagated by cleavage. The second transient was planned to produce a deep cleavage crack jump with an arrest or mode conversion occurring only after conditions conducive to unstable tearing were attained. In the first transient PTSE-2A, ductile tearing occurred in three separate phases: (1) prior to warm prestressing; (2) during reloading; and (3) after the cleavage arrest. The crack propagated both axially and radially by cleavage. In the second transient PTSE-2B, K_I increased monotonically, while the crack tore stably, propagated radially in cleavage, and then tore unstably.

In the elastodynamic analyses of the transients observed in PTSE-2, a 2-D plane strain finite-element formulation was utilized to model the test vessel. The finite element model employed in these analyses is depicted in Fig. 2 and consists of 2114 nodes and 671 eight-noded isoparametric elements. Constant material properties are given by Young's modulus E = 202.3 GPa, Poisson's ratio ν = 0.3, thermal expansion coefficient α = 1.44×10^{-5}/°K and density ρ = 7833 kg/m^3. Measured values of the radial

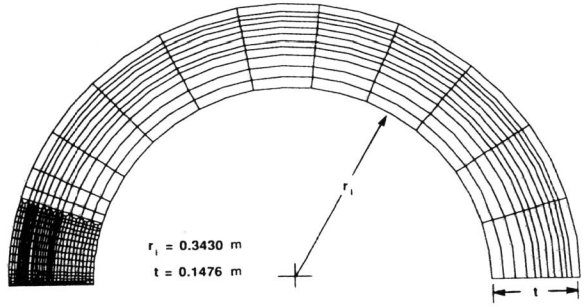

Fig. 2. Finite element model for posttest elastodynamic fracture analysis of PTSE-2.

temperature distribution and internal pressure at the time of cleavage crack propagation in the transient of PTSE-2 are given by Bryan et al., (1987); the boundary conditions are assumed constant during the run-arrest event. The time step Δt for the dynamic analyses was fixed at Δt = 0.2 μs.

Results from application-mode elastodynamic analyses of the A and B transients are depicted in Figs. 3 and 4 and in Table 3. Figure 3 gives the computed crack-depth ratio, a/w, as a function of time for each of the two

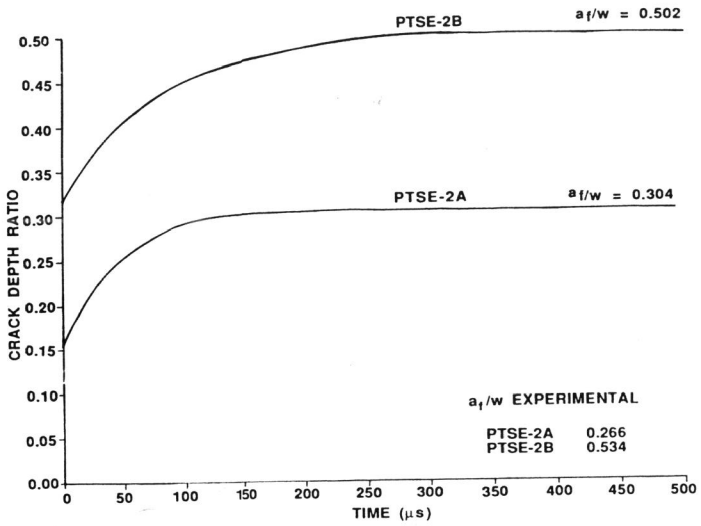

Fig. 3. Crack-depth ratio versus time for posttest elastodynamic analysis of PTSE-2.

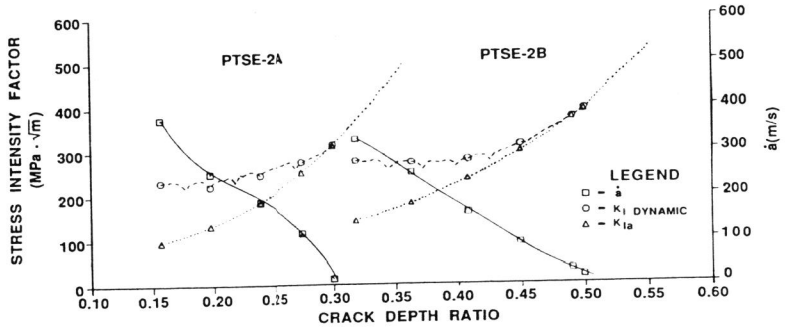

Fig. 4. Stress-intensity factor, crack-velocity, and static crack-arrest toughness versus crack-depth ratio for posttest elastodynamic analysis of PTSE-2.

Table 3. Initiation and arrest parameters from posttest elastoplastic and elasto-dynamic analyses of PTSE-2

Experiment phase	a/w	a (m)	Temperature (°C)	K_I (MPa$\sqrt{m}$)	Event
PTSE-2A					
S[a]	0.1524	0.0225	80.7	198.9	Initiation
ES[b]	0.1524	0.0225	80.7	238.4	Initiation
S	0.2663	0.0393	130.6	261.4	Arrest
ED[c]	0.3040	0.0449	145.6	313.8	Arrest
PTSE-2B					
S	0.3123	0.0461	102.4	248.1	Initiation
ES	0.3123	0.0461	102.4	284.5	Initiation
S	0.5339	0.0788	162.9	419.3	Arrest
ED	0.5016	0.0740	155.4	393.2	Arrest

[a] S = quasi-static elastoplastic analyses (Bryan et al., 1987) based on measured crack depth.

[b] ES = quasi-static elastic analysis (present study).

[c] ED = application-mode elastodynamic analysis (present study).

transients and compares computed values with measured data at crack arrest. Figure 4 depicts the dynamic stress-intensity factor K_I, the crack velocity $\dot{a}$, and the static crack-arrest toughness K_{Ia} vs a/w relations for the transients, and it indicates that the crack propagates into a rising K_I field for both run-arrest event. Table 3 compares selected results obtained from previously reported 2-D quasi-static elastoplastic analyses (Bryan et al., 1987) based on measured crack depths and from the quasi-static elastic and elastodynamic analyses of the present study. The differences in computed K_I values at initiation in the two transients are due primarily to plasticity effects that are not modelled in this study.

The computed results presented in Figs. 3 and 4 represent contrasts in the predicted kinematic behavior of the crack tip during the two transients of PTSE-2. In the A transient, the computed crack-tip velocity falls rapidly to zero at time t ≈ 150 μs following initiation of the cleavage event. Calculations for the B transient indicate that the crack velocity was non-zero for a longer period of time, at least 300 μs. The cleavage event observed in the B transient was interrupted by a narrow band of ductile tearing at a/w ≈ 0.47 that extended the entire length of the crack. Post-test studies of the fracture surface indicate that cleavage was still occurring over short discontinuous segments of this tearing band, and that the crack eventually reinitiated in cleavage and arrested at a/w = 0.534. Although the complex interactions of these fracture modes are not modelled in the present study, results in Fig. 4 show that a small increase in the K_{Ia} curve could produce an arrest at the approximate location of the ductile tearing band. No such interruption of the A transient cleavage event by tearing was detected, and the computed results in Fig. 4 are consistent with that observation.

CONCLUSION

Application-mode elastodynamic analysis results presented here for PTSE-2 are qualitatively consistent with some of the fracture events observed in the two transients of PTSE-2. However, comparisons of results from 2-D quasi-static linear-elastic and elastoplastic analyses (Table 3) of the PTSE-2 transients indicate that calculated fracture parameters are significantly influenced by the incorporation of plasticity into the computational models. The latter results are due primarily to effects of the relatively low tensile strength of the PTSE-2 test material (see Table 2). By contrast, inelastic effects were found not to be significant for the PTSE-1 test transients; furthermore, static and dynamic analyses of PTSE-1 based on linear-elastic fracture mechanics models showed little difference and were in agreement with measurements of arrested crack depth (Bryan et al., 1986; Bass et al., 1987). Work is currently under way at ORNL to perform dynamic analyses of PTSE-2 that take into account the effects of plasticity and of the sequence of stable ductile tearing and cleavage events observed in both transients of the test.

REFERENCES

Bass, B. R., C. E. Pugh, and J. K. Walker (1987). "Elastodynamic Fracture Analysis of Large Crack-Arrest Experiments," *Nuclear Engineering and Design*, Vol. 98, 157—169.

Bass, B. R., C. E. Pugh, J. Keeney-Walker, and C. W. Schwartz (1988). "Late-Event Viscoplasticity in Wide-Plate Crack Arrest Tests," *International Journal of Pressure Vessels and Piping*, Vol. 31, 325—348.

Bass, B. R., C. E. Pugh, J. G. Merkle, D. J. Naus, and J. Keeney-Walker (1988). "Fracture Analyses of Heavy-Section Steel Technology Wide-Plate Crack-Arrest Experiments," *Fracture Mechanics: Nineteenth Symposium*, ASTM STP-969, T. A. Cruse (Ed), American Society for Testing Materials, Philadelphia, Pa., 691—733.

Bathe, K. J. (1984). *ADINA — A Finite Element Program for Automatic Dynamic Incremental Nonlinear Analysis*, Report AE 84-1, Massachusetts Institute of Technology, Cambridge, MA.

Bryan, R. H., B. R. Bass, J. G. Merkle, C. E. Pugh, G. C. Robinson, and G. D. Whitman (1986). "The Heavy-Section Steel Technology Pressurized-Thermal-Shock Experiment, PTSE-1," *Engineering Fracture Mechanics*, Vol. 23, No. 1, 81—97.

Bryan, R. H., B. R. Bass, S. E. Bolt, J. W. Bryson, W. R. Corwin, J. G. Merkle, R. K. Nanstad, and G. C. Robinson (1987). *Pressurized-Thermal-Shock Test of 6-in.-Thick Pressure Vessels. PTSE-2: Investigation of Low Tearing Resistance and Warm Prestressing*, NUREG/CR-4888 (ORNL-6377), Martin Marietta Energy Systems, Inc., Oak Ridge Natl. Lab.

Fedderson, C. F. (1967). *Current Status of Plane Strain Crack Toughness Testing of High-Strength Metallic Materials*, Crack Arrest Methodology and Applications, ASTM STP-410, American Society for Testing and Materials, Philadelphia, Pa.

Naus, D. J., B. R. Bass, J. Keeney-Walker, R. J. Fields, R. deWit, and S. R. Low (1988). "Summary of HSST Wide-Plate Crack-Arrest Tests and Analyses," *Proc. of U.S. Nuclear Regulatory Commission Fifteenth Water Reactor Safety Information Meeting held at National Bureau of Standards*, Gaithersburg, Maryland, NUREG/CP-0091, 17—40.

Tada, R., P. C. Paris, and G. R. Irwin, (1973). *The Stress Analysis of Cracks Handbook*, Del Research Corp., Hellertown, Pa.